# Malaysian Journal of Analytical Sciences (MJAS) Published by Malaysian Analytical Sciences Society

## THE ELECTROCHEMICAL BEHAVIOUR OF Au-PEDOT/rGO MODIFIED ELECTRODE IN URIC ACID

(Sifat Elektrokimia Elektrod Bermodifikasi Komposit Au-PEDOT/rGO dalam Asid Urik)

Farhanini Yusoff<sup>1</sup>\*, Mohd Faris Rosdidi<sup>1</sup>, Azleen Rashidah Mohd Rosli<sup>1</sup>, Syara Kassim<sup>2</sup>, Noor Aniza Harun<sup>2</sup>, Noorashikin Md Saleh<sup>3</sup>

<sup>1</sup>Faculty of Science and Marine Environment

<sup>2</sup>Advanced Nano Materials (ANoMa) Research Group, Faculty of Science and Marine Environment

Universiti Malaysia Terengganu, 21030 Kuala Nerus, Terengganu, Malaysia

<sup>3</sup>Research Centre for Sustainable Process Technology, Department of Chemical Engineering,

Faculty of Engineering and Built Environment,

Universiti Kebangsaan Malaysia, 43600 UKM Bangi, Selangor, Malaysia

\*Corresponding author: farhanini@umt.edu.my

Received: 28 March 2021; Accepted: 23 May 2021; Published: 27 June 2021

#### **Abstract**

The development of gold nanoparticle/poly(3,4-ethylene dioxythiophene)/reduced graphene oxide (denoted as Au-PEDOT/rGO) sensor is necessary for the detection of UA as the irregular amount of UA in the human body may cause several diseases such as gout, heart disease, kidney stone and hypertension. In this work, Au-PEDOT/rGO nanocomposite was synthesized by a facile chemical technique. The morphology, composition, and structure of Au-PEDOT/rGO composite were confirmed by FTIR, SEM, and XRD characterization. FTIR spectrum showed the presence of C-O-C stretching and C-S stretching of the thiophene ring. The attachment of Au with PEDOT and rGO was confirmed by SEM. XRD analysis showed the presence of Au(111), Au(200), Au(220), Au(311) and Au(222) corresponding to Au-PEDOT/rGO composite. This proved that Au-PEDOT/rGO has been successfully synthesized. The electrochemical behavior of Au-PEDOT/rGO/GCE was evaluated by cyclic voltammetry (CV) in 1.0 M KCl with 5 mM K4[Fe(CN)6] and the results demonstrated that Au-PEDOT/rGO/GCE has a better electrical conductivity for detection of UA in the real sample. DPV measurements showed a linear relationship between oxidation peak current and concentration of UA in phosphate buffer (pH 7) over the concentration range 0.10 μM until 25.0 μM. The limit of detection of UA is 0.05 μM, and the limit of quantification of UA is 0.22 μM. Thus, Au-PEDOT/rGO electrode composite is a worthy alternative for the detection of UA in human's urine.

Keywords: conducting polymer, gold nanoparticles, reduced graphene oxide, uric acid

#### Abstrak

Pembangunan sensor buat zarah nano aurum/poli(3,4-etilenadioxitiofena/grafin oksida terturun (dilabel sebagai Au-PEDOT/rGO) adalah diperlukan untuk pengesanan UA kerana jumlah UA yang tidak normal dalam tubuh manusia boleh menyebabkan beberapa kondisi penyakit seperti gout, penyakit jantung, batu ginjal dan darah tinggi. Dalam kajian ini, komposit nano Au-PEDOT/rGO

### Farhanini et al: THE ELECTROCHEMICAL BEHAVIOUR OF Au-PEDOT/rGO MODIFIED ELECTRODE IN URIC ACID

telah disinthesis melalui teknik kimia mudah. Morfologi, komposisi, dan struktur komposit Au-PEDOT/rGO telah disahkan melalui teknik pencirian FTIR, SEM, dan XRD. Spektrum FTIR menunjukkan kehadiran regangan C-O-C dan regangan C-S bagi ikatan tiofena manakala penggabungan Au kepada lembaran PEDOT dan rGO telah dibuktikan melalui SEM. Analisis XRD menunjukkan kehadiran Au(111), Au(200), Au(220), Au (311) dan Au(222) sepadan dengan komposit Au-PEDOT/rGO. Keputusan tersebut telah mengesahkan bahawa Au-PEDOT/rGO telah berjaya disintesis. Sifat elektrokimia Au-PEDOT/rGO telah dinilai melalui voltammetri berkitar (CV) di dalam 1.0 M KCl bersama dengan 5 mM K4[Fe(CN)6] dan hasil kajian menunjukkan bahawa Au-PEDOT/rGO memiliki konduksi elektrik yang bagus untuk pengesanan UA di dalam sample nyata. Analisis DPV menunjukkan hubungan linear antara puncak pengoksidaan arus dan kepekatan UA di dalam penimbal fosfat (pH 7) diantara julat kepekatan 0.10 μM hingga 25.0 μM. Had pengesanan yang diukur bagi UA ialah 0.05 μM manakala had pengukuran UA adalah 0.22 μM. Oleh itu, komposit Au-PEDOT/rGO merupakan alternatif yang berbaloi untuk mengesan UA dalam air kencing manusia.

Kata kunci: polimer pengalir, zarah nano aurum, grafin oksida terturun, asid urik

#### Introduction

Uric acid (UA) is a purine end product formed by xanthine dehydrogenase in humans, and it has been discovered to play a significant role in the physiology of living organisms [1]. The two types of purine are exogenous and endogenous. The exogenous pool of purine is related to diet and animal proteins, while the endogenous purine metabolism that produces UA is from the liver, intestines, and other body tissues [2]. In theory, UA has either benefit or drawback effect toward the human body depending on concentration intake. Hyperuricemia that refers to overproduction or underexcretion of UA can lead to serious health issues such as heart disease, kidney stone, and gout [3]. These diseases are linked to chronic diseases such as hypertension, diabetes, metabolic syndrome, and renal failure [4]. The most common clinical features of hyperuricemia are associated with crystallization and uric acid deposition in surrounding joints and tissues. However, the precise mechanism of tissue injury caused by uric acid remains indefinite. Overproduction of UA also causes oxidative stress. Thus, this detection of UA will benefit not only the field of clinical diagnosis but also the human health.

Several methods of sensing UA in the human body have been discovered over the past years such as High Performance Liquid Chromatography (HPLC) [5], enzymatic [6], electrochemical [7] and phosphortungstic acid deoxidizing methods [8]. However, the electrochemical method is most favorable due to its fast analysis, low detection limit, sensitivity, and also high in accuracy compared to the other methods. UA often coexists with the presence of ascorbic acid (AA), and

dopamine (DA) in the human urine sample and these substances are electrochemically active substances that will interfere in the process of UA detection [9]. Thus, electrode surface modification is an effective alternative to overcome these problems as the bare electrode is found to have challenges in separating the peak of interference substance [10].

Graphene which is a thin sheet of hexagonally arranged carbon has captivate significant attention because of its exclusive thermal, optical and also its electrical characteristics. Graphene undergoes oxidation and exfoliation forming graphene oxide, which contains some reactive oxygen [11]. The immensely improved graphene oxide's surface ability makes it easier to bind with other compounds due to the oxygen-containing group [12].

Meanwhile, poly(3,4-ethylene dioxythiophene), also known as PEDOT, is one of the electroactive polymers that is widely studied because of its stability in the environment and enormous conductivity of its polycationic form [13]. This polymer is used for numerous applications as it possesses a simple synthesis process, superior biocompatibility and relatively wide electrical conductivity [10,14]. Recently, researches on noble metal nanoparticles such as platinum, gold, and silver were actively conducted due to their properties in conductivity and electrocatalyticity [15]. Gold (Au) nanoparticle has good prospects in the application of the detection of electroactive species [16]. Its specific structure, low toxicity, and biocompatibility make it compatible in sensing application [17].

Herein, we reported an electrocatalyst of Au decorated PEDOT functionalized with rGO (Au-PEDOT/rGO) which was synthesized by the facile synthesis technique. Then, the modified electrode was prepared via the drop-casting of the composite onto the surface of a glassy carbon electrode (GCE). The performance of the electrode as an electrochemical sensor for the detection of UA was evaluated using Cyclic Voltammetry (CV). The unique Au-PEDOT/rGO sensor is revealed to have a wide linear response over the concentration range from 0.1 to 25.0 µM UA. Additionally, detection of UA in a human urine sample is found to exhibit high accuracy. This newly developed sensor is expected to offer high accuracy, high sensitivity with fast analysis towards the determination of UA.

#### **Materials and Methods**

#### **Materials**

3,4-ethylenedioxythiophene (EDOT), gold(III) chloride hydrate (HAuCl<sub>4</sub>), sodium borohydride (NaBH<sub>4</sub>), sodium nitrate (NaNO<sub>3</sub>), graphite, Uric acid (UA), ethanol absolute (EtOH), potassium chloride (KCl) and potassium hexacyanoferrate(II) 3-hydrate (K<sub>4</sub>Fe(CN)<sub>6</sub>) powder were purchased from Sigma-Aldrich, USA. Meanwhile, di-potassium hydrogen phosphate (K<sub>2</sub>HPO<sub>4</sub>), potassium dihydrogen phosphate (KH<sub>2</sub>PO<sub>4</sub>), potassium permanganate (KMnO<sub>4</sub>), and aluminium oxide (Al<sub>2</sub>O<sub>3</sub>) were purchased from Merck, Germany. The UA standard solution was prepared in the 0.1 M of phosphate buffer solution.

#### Synthesis of rGO

Graphene oxide (GO) was synthesized from graphite powder via a modified Hummer's method, which was previously reported by Kaur *et al.*, 2018 [18]. Then, 200 mg of GO solution from the previous product was added into 200 ml of deionized water (DI) and sonicated for 2 hours. Next, 66.8 μL of hydrazine hydrate was added into the mixture with ratio of 1:3 (hydrazine: GO). The beaker was immersed in an oil bath at 80°C under cooled condenser for 12 hours. The solution was then transferred into 50 mL centrifuge tube and centrifuged at 3500 rpm for 10 minutes. The supernatant from the centrifuge process was removed and EtOH was added into the centrifuge tube to further centrifuge the solution. This step was repeated for three times and product was

then washed with DI water to remove excess impurities. Lastly, the product was filtered by a vacuum pump and dried at 60°C for 12 hours.

#### Preparation of Au/rGO

About 4 mL of rGO was added into 25 mL of HAuCl<sub>4</sub> solution (0.2 mg mL<sup>-1</sup>). The mixture was stirred for 1 hour in order to encourage the interaction between the graphene surface with the gold ions. 0.2 mol/mL of sodium citrate was dropped gradually into the mixture. Next, the solution was heated at 80°C for 2 hours [19]. The solution was then transferred into 50 mL centrifuge tube for centrifugation process at 3500 rpm for 10 minutes. The supernatant was removed then EtOH was added and centrifuge at 3500 rpm for 10 minutes. After 3 times removal of the excess supernatant, the product was resuspended by washing with deionized water via centrifugation. The product was filtered by vacuum pump and dry in oven at 60°C for 12 hours.

#### Preparation of Au-PEDOT/rGO

Approximately 70 mL of 0.65 mM HAuCl<sub>4</sub> solution was added into the mixture of 5 mL ethanol solution and 22.5 mM EDOT while stirred at the normal room temperature. The formation of PEDOT was occurred when the mixture colour changes from black-colored solution to dark blue and AuCl<sub>4</sub>- ions as the oxidant was reduced to form Au nanparticles [10]. The reaction was then kept stir for 4 hours. Later, the 0.5 mg/mL rGO suspension was mixed into the solution and then, the mixture was sonicated for 2 hours in order to disperse the Au-PEDOT and rGO. Lastly, the obtained solution was centrifuged by transfer the solution into the centrifuge tube and washed with EtOH and distilled water repeatedly until a neutral pH.

#### Characterization of Au-PEDOT/rGO

The characterization of Au-PEDOT/rGO was determined by using Fourier Transform Infrared Spectrometer (FTIR) for determination of the functional group and Scanning Electron Microscopy (SEM) was used to study the surface morphology and structure of the composite samples. Meanwhile, X-ray Diffractometry (XRD) was practiced for determation of the atomic and molecular structure of a crystal and UV-Vis spectroscopy is used to indicate the bond

transition of the sample. A standard three electrode electrochemical cell was used to carry out the electrochemical measurements in which a platinum wire act as auxiliary electrode, glassy carbon electrode (GCE) as working electrode and reference electrode of Ag/AgCl. The cyclic voltammetry was obtained in  $5\mu$ M K<sub>4</sub>[Fe(CN)<sub>6</sub>] and 1 M KCl at different scan rates in the potential range of -0.2 to 0.8 V at room temperature.

#### Fabrication of Au-PEDOT/rGO/GCE

Before the surface modification of the bare glassy carbon electrode (3 mm in diameter), the surface was polished with fine alumina slurry (0.05  $\mu$ m) and rinse thoroughly with deionized water. The GCE was then ultra-sonicated in the acetone and deionized water successively and dry under ambient condition. The Au-PEDOT/rGO (1.0 mg) was added into 1 mL of deionized water and produced a homogeneous suspension after completion of one-hour sonication. Finally, 5  $\mu$ L of the Au-PEDOT/rGO homogenized solution was drop-casted on the pretreated GCE and allowed to dry in a vacuum desiccator for 2 hours.

#### **Determination of UA**

0.05 M of phosphate buffer solution (PBS saline) was prepared by mixing the two substance of 8.41 g of potassium dihydrogen phosphate (KH<sub>2</sub>PO<sub>4</sub>) and 6.63 g of di-potassium hydrogen phosphate (K<sub>2</sub>HPO<sub>4</sub>). The UA standard solution was then prepared by dissolving the UA standard powder with the PBS saline prepared previously. Then, differential pulse voltammetry (DPV) technique was practiced to obtain the oxidation peak of the UA (concentration ranging from 0.1  $\mu$ M to 25.0  $\mu$ M) through voltammograms. The voltammogram analysis were then used to plot a calibration curve, and the analysis was used as an indicator to determine the lowest detection of UA.

#### **Results and Discussion**

#### FTIR and XRD analyses

Figure 1 shows the FTIR spectra of graphite powder, GO, rGO, Au/rGO, and Au-PEDOT/rGO. From the figure, no significant peaks are observed for raw graphite. However, the GO spectrum showed a peak at 1051cm<sup>-1</sup>, which is attributed to the C-O bond, indicating that GO was successfully oxidized by the

graphite. The peak at 1620 cm<sup>-1</sup> was appointed to the alkene group C=C stretching and the 1724 cm<sup>-1</sup> indicated C=O stretching. A broad peak at 3392 cm<sup>-1</sup> indicated O-H stretching vibrations of C-OH groups. As expected, rGO bands are relatively weaker as it was reduced from GO to rGO by hydrazine hydrate. The intensities of oxygen-containing functional group absorption bands such as C-O at 1564 cm<sup>-1</sup> and O-H stretchings at 3417 cm<sup>-1</sup> are dramatically reduced. Also found to have disappeared from the rGO composites were the C=O and C=C stretchings. This shows that after the reduction process, rGO was successfully obtained.

Accordingly, the intent for the reduction of GO was to remove the epoxy and hydroxyl groups on the spectra, while other functional groups such as carbonyl, carboxyl and ester groups present on the edges of the carbon plane do not interfere with the conductivity of the rGO sheet. For the FTIR spectrum of Au/rGO, the peak present at 3466 cm<sup>-1</sup> is linked to the stretching of O-H. The 1575 cm<sup>-1</sup> absorption peak represents epoxide C-O vibration. There are no additional Au peaks detected, but due to Au doping on rGO, the intensity is increased. Therefore, the spectrum of Au/rGO should correspond to rGO composite. However, for the FTIR spectrum of Au-PEDOT/rGO, the vibrational band at 1512 cm<sup>-1</sup> was due to the formation of C=C and the absorption peak at 1346 cm<sup>-1</sup> is assigned to the C-C stretching in the ethylene dioxy group of the thiophene ring structure [20]. The C-S bond in the thiophene ring appeared at the wavenumber of 975 cm<sup>-1</sup> and 840 cm<sup>-1</sup>.

The XRD patterns for GO, rGO, Au/rGO, and Au-PEDOT/rGO are illustrated in Figure 2. The diffractogram of characteristic peak of GO was observed at  $10.25^{\circ}$  that represents a wider interlayer distance between the GO layers. This is the result of the oxidation of graphite during the synthesis process and also due to the formation of certain functional groups such as epoxy, carboxyl and hydroxyl which is supported in the FTIR results [21]. Meanwhile, the XRD pattern of rGO showed a broad diffraction peak at  $2\theta = 23.0^{\circ}$  due to the removal of oxygen functional group from GO which indicated that the rGO was successfully obtained. According to the XRD pattern of Au/rGO composites,

diffraction peaks at  $2\theta = 38.2^{\circ}$ ,  $44.45^{\circ}$ ,  $65.61^{\circ}$ ,  $77.61^{\circ}$ , and  $82.61^{\circ}$  are indexed to the (111), (200), (220), (311), and (222) planes of well crystalline Au with cubic phase. The diffraction peak corresponds to 002 from rGO layers and is complimented by a broad graphitic peak that appears at  $2\theta = 23^{\circ}$ . The diffractogram of AuNP-PEDOT/rGO showed similar pattern and diffraction peaks with Au/rGO showed more intense  $2\theta$  peak. The  $2\theta$  peak appeared at  $38.05^{\circ}$ ,  $44.17^{\circ}$ ,  $64.52^{\circ}$ ,  $77.30^{\circ}$  and  $81.84^{\circ}$ , which corresponded to the reflection planes of Au (111), Au (200), Au (220), Au (311) and Au (222), respectively. Furthermore, a broad diffraction peak at  $23.0^{\circ}$  belonging to C (002) from PEDOT and rGO was also observed [22]. This proved that metallic gold appeared in AuNPs/PEDOT/rGO sheets.

#### **SEM** analysis

SEM was utilized to observe the morphology of graphite, GO, rGO, Au/rGO, and Au-PEDOT/rGO. It provided a highly magnified image of the composite surface. Figure 3a shows the image of graphite (at

5000X magnification) which is as platelet-like crystalline form of carbon. It could be clearly seen that graphite was arranged and presented as a typical multilayer structure in agglomerates. However, GO (Figure 3b) showed the wrinkled aggregates composite with multiple folds which is related to the oxidation process to promote oxygen-containing functional groups on the graphite sheets. The formation of rGO (Figure 3c) produced more rough wrinkles compared to GO. This is due to the reduction process by hydrazine hydrate. In Figure 3d, Au particles were uniformly distributed across the rGO. As compared to the rGO micrograph, the Au nanoparticles were seen to be successfully incorporated and covered the rGO surface. Meanwhile, the bubble-like shape (Figure 3e) indicates that the Au/PEDOT particle displayed an irregular shape and uniformly wrapped the rGO sheet. The wrinkled sheet of rGO provided an attachment site for Au along with PEDOT particle [23].

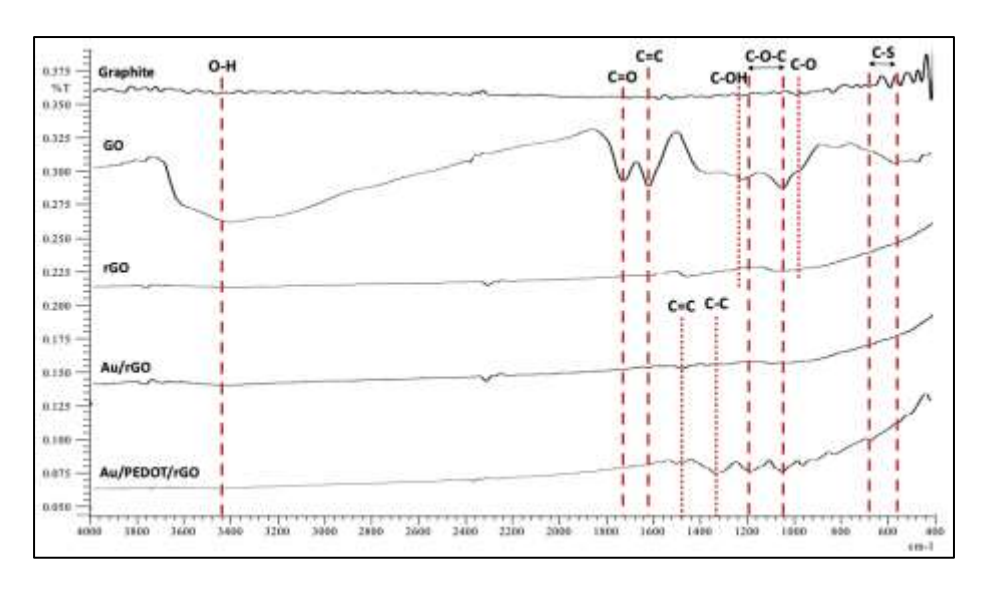


Figure 1. FTIR spectra measured of graphite, GO, rGO, Au/rGO and Au-PEDOT/rGO electrocatalyst

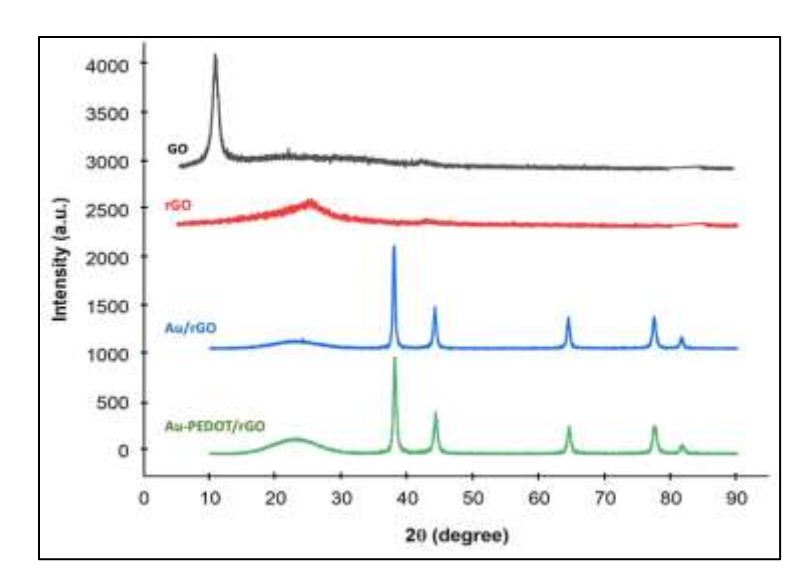


Figure 2. XRD pattern of GO, rGO, Au/rGO and Au-PEDOT/rGO

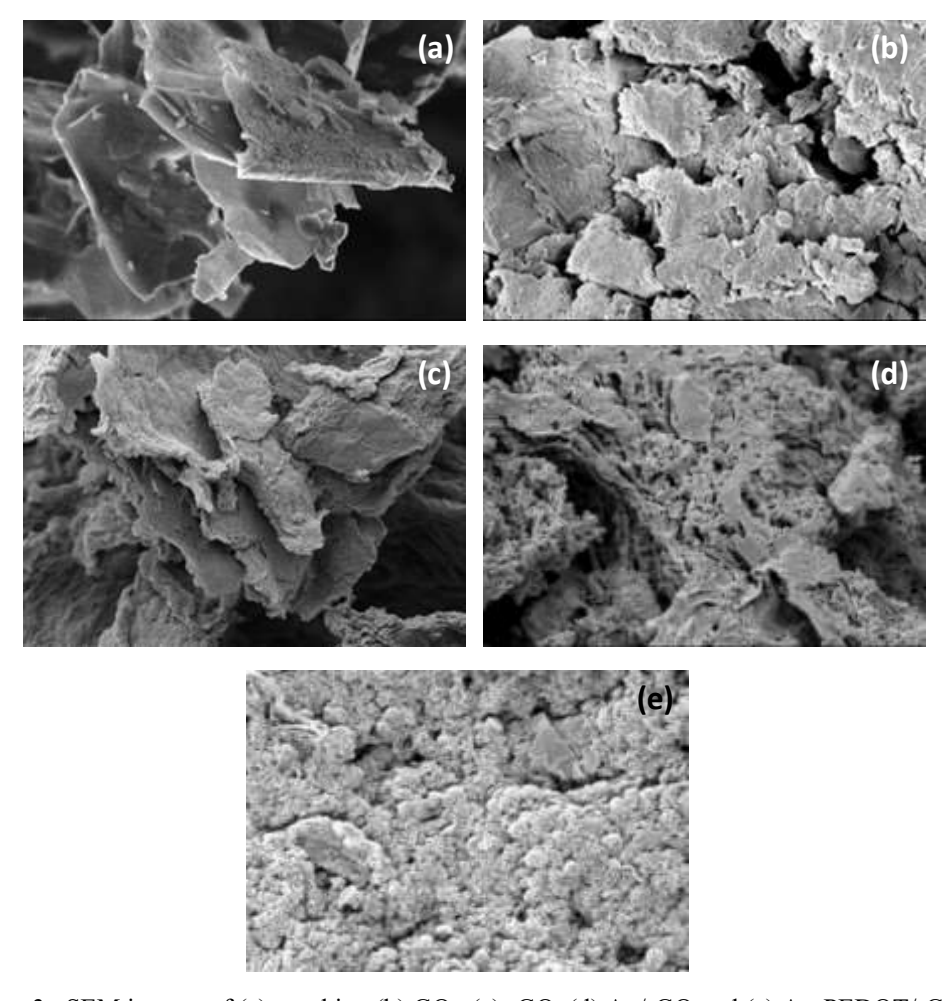


Figure 3. SEM images of (a) graphite, (b) GO, (c) rGO, (d) Au/rGO and (e) Au-PEDOT/rG

#### **UV-Vis analysis**

Figure 4 shows the UV-visible spectra of rGO, Au/rGO, and Au-PEDOT/rGO while Figure 4: Inset shows the comparison of UV spectrum of all composites with the presense of GO. The UV-visible spectrum of GO had the highest absorption peak at 228 nm indicating the  $\pi$ - $\pi$ \* transition C=C aromatic bonds [24]. As for rGO, the absorption peak had been reduced which proves the reduction process of rGO by hydrazine hydrate. Au/rGO had absorption peaks at 268 nm and 525 nm, while Au-PEDOT/rGO showed an absorption peaks of 226 nm and 510 nm. The formation of gold nanoparticles decorated on the rGO surface was demonstrated by the broad absorption peak observed for Au/rGO and Au-PEDOT/rGO at 510 nm and 525 nm, respectively, due to the active surface plasmon resonance of Au particle. The lowest absorbance represents the simultaneous reduction of Au<sup>3+</sup> to Au as well as reduction of GO to rGO resulting in Au/rGO and Au-PEDOT/rGO.

#### **Electrochemical characterization**

A cyclic voltammetry technique exploiting the solution based redox probe [Fe(CN)<sub>6</sub>]<sup>4</sup> was used to analyze the electrochemical features of the modified electrode as shown in Figure 5a. In theory, the CVs of all four modified electrodes (GO/GCE, rGO/GCE, Au/rGO/GCE, and Au-PEDOT/rGO/GCE) were expected to show higher in redox peak current and smaller peak separation compared to bare GCE. In these cases, Au-PEDOT/rGO showed the higher redox peak current than bare, GO, rGO and Au/rGO modified electrodes and enhanced electron transfer between the electrode surface and electrolyte that showed a high electron transfer of composite Au-PEDOT/rGO compared to other modified electrodes studied.

To further investigate the behaviour of Au-PEDOT/rGO modified electrode, the effect of current toward different scan rates was also examined (Figure 5b). From this figure, the oxidation peak current increased proportionally with scan rate. This finding can be explained by the limited electron transfer process of the system. The diffusion layer in a slow voltage scan rate will grow much farther from the electrode in comparison to a fast scan rate. Furthermore, the peak separation remaining at the same value shows a perfect reversibility

of electrode [12]. The result obtained also shows that the redox peak current increased linearly with the square root of scan rate (Figure 5c) indicating that redox reaction was controlled by the diffusion of [Fe(CN)6]<sup>-3/-4</sup> towards the electrode surface. According to the Randles-Sevcik formula (Equation 1), it can be clearly seen that the Ipa and Ipa increases against square roots of scan rate with a linear correlation coefficient of  $(r^2) = 0.9893$  and 0.9887, respectively where  $I_p$  is the oxidation peak current (A), n is the number of transferred electrons per mole, A is the active surface area of the electrode (cm<sup>2</sup>), D is the diffusion coefficient (cm<sup>2</sup>/sec), C is concentration (mol/cm<sup>3</sup>) and v is the scan rate (V/s). These results indicated that the redox reaction of [Fe(CN)6]-3/-4 on Au-PEDOT/rGO/GCE surface is a diffusion-controlled electrochemical processes.

$$I_{p} = (2.69 \times 10^{5}) n^{3/2} A D^{1/2} C v^{1/2}$$
 (1)

#### Electrochemical oxidation of UA at Au-PEDOT/rGO modified GCE

Electrochemical oxidation of 1 mM of UA was conducted on a bare GCE and Au-PEDOT/rGO modified GCE by CV to elucidate their electron transfer behavior in the presence of PBS (0.1 M) at a scan rate of 50 mVs<sup>-1</sup> and potential range in -0.2 V to 0.8 V (Figure 6). The Au-PEDOT/rGO/GCE demonstrated an immensely enhanced oxidation peak at potential of 0.45 V. In contrast, oxidation at the bare GCE showed a lower oxidation peak current at the same potential. It was obvious that Au-PEDOT/rGO/GCE produced highly enhanced catalytic current of UA oxidation compared to the bare GCE which can be attributed to the synergistic effect of the individual component in the nanocomposite, promoting the electron transfer between the redox probe and the electrode surface. This establishes that Au-PEDOT/rGO/GCE exhibit high electro-catalytic activity useful for UA detection. Figure 6 (inset) depicts a potential reaction for the oxidation of UA at the Au-PEDOT/rGO/GCE modified GCE. The oxidation of UA is a direct two-electron transfer mechanism where the 1H-purine-2,6,8 (9H)trione was converted by 1H-purine-2,6,8 (3H,7H,9H)trione which is also known as uric acid.

#### **Determination of UA by DPV**

DPV has much higher current sensitivity than the CV and therefore, lower UA concentrations can be analysed more accurately. The concentrations of UA ranging from 0.1  $\mu$ M to 25.0  $\mu$ M at the Au-PEDOT/rGO /GCE modified electrode in 0.1 M PBS solution are shown in Figure 7a. It was observed that the peak current increased with the increase in concentration. Figure 7b represents a linear calibration plot between peak current and concentration for the uric acid in the given range and gave the linear regression equation of  $y = 0.8915x + 10^{-1}$ 

2.647, with an  $r^2$  value of 0.9974. The limit of detection (LOD) for UA sample by using Au-PEDOT/rGO/GCE was calculated to be 0.05  $\mu M$  while the limit of quantification (LOQ) was determined to be 0.22  $\mu M$ . The synergistic effect of Au-PEDOT and rGO for the sensitive detection of UA could be contributed to the outstanding electrocatalytic performance. For UA detection, this potential modified electrode was compared to other similar electrodes, as shown in Table 1.

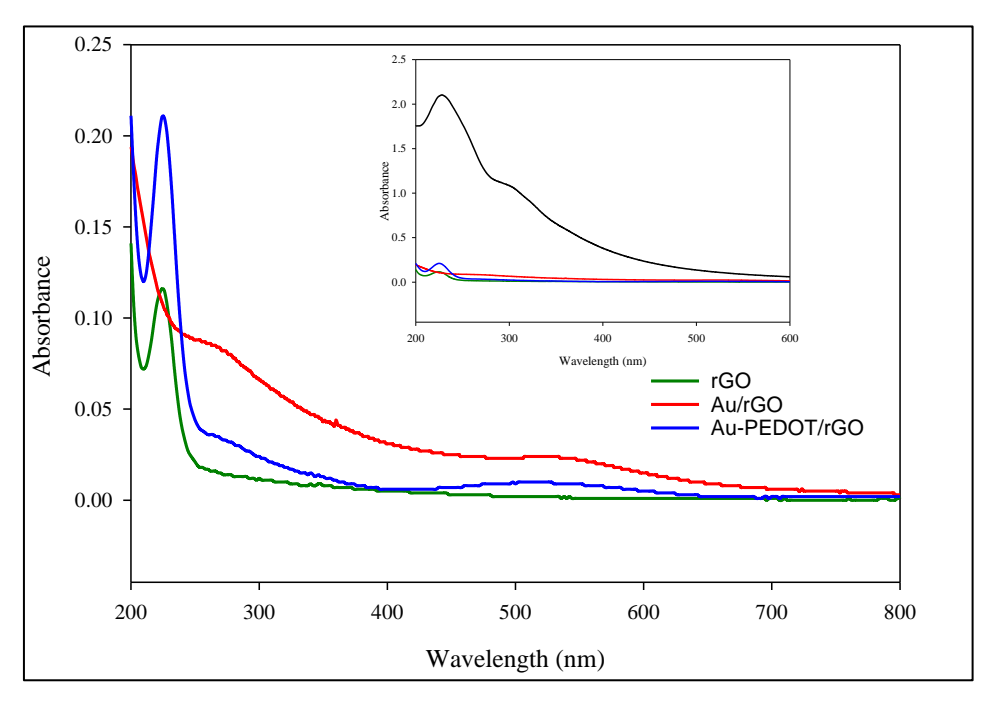


Figure 4. UV spectra of rGO, Au/rGO and Au-PEDOT/rGO. Inset: Comparison of UV spectra of all composites with the presence of GO (black line)

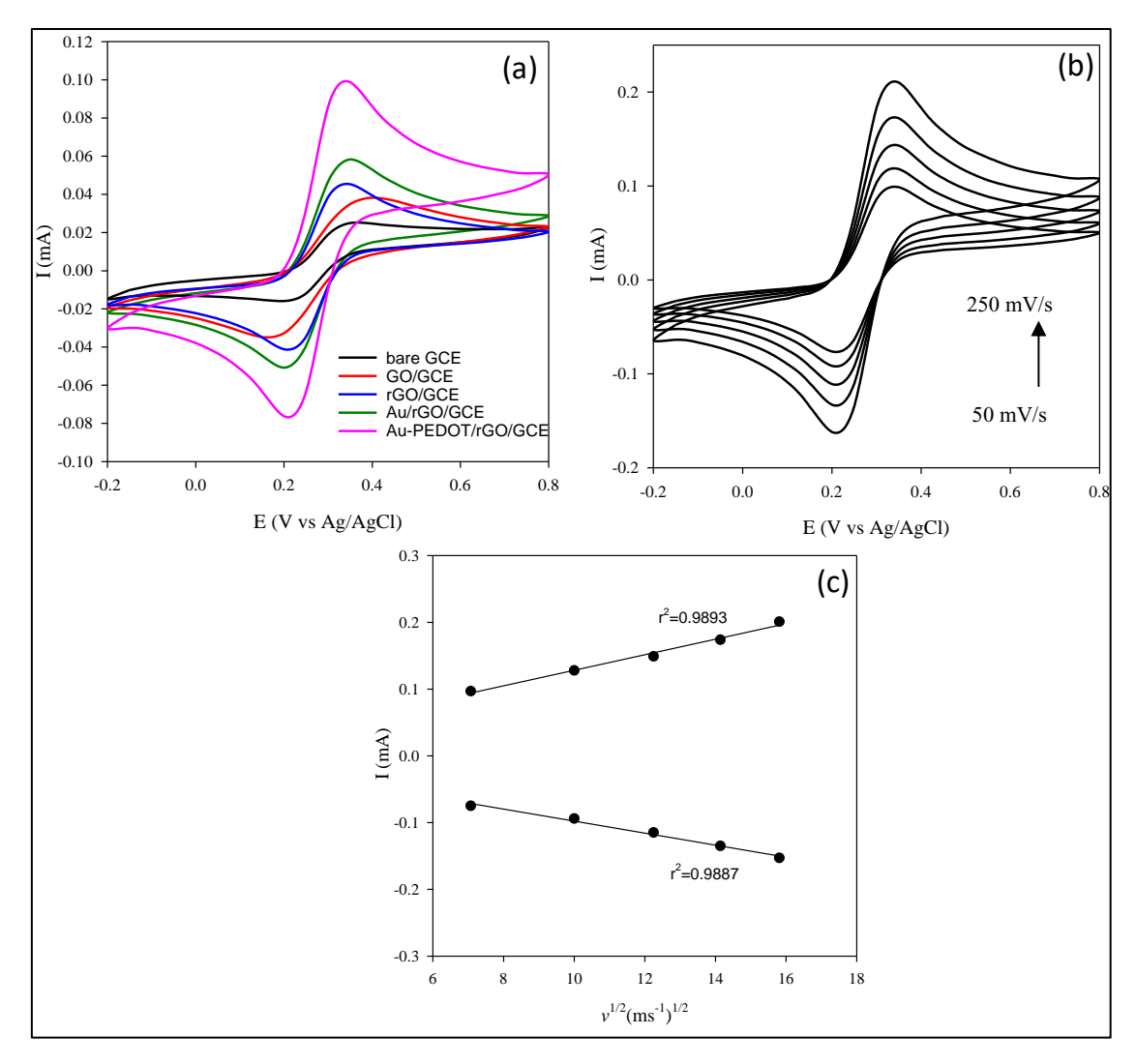


Figure 5. (a) Cyclic voltammogram of modified electrode in  $5\mu M$  K<sub>4</sub>[Fe(CN)<sub>6</sub>] and 1 M KCl electrolyte solution with scan rate of 100 mV/s, (b) Cyclic voltammograms of Au-PEDOT/rGO/GCE at different scan rate in  $5\mu M$  K<sub>4</sub>[Fe(CN)<sub>6</sub>] and 1 M KCl electrolyte solution and (c) The plot of square root of scan rate vs. current

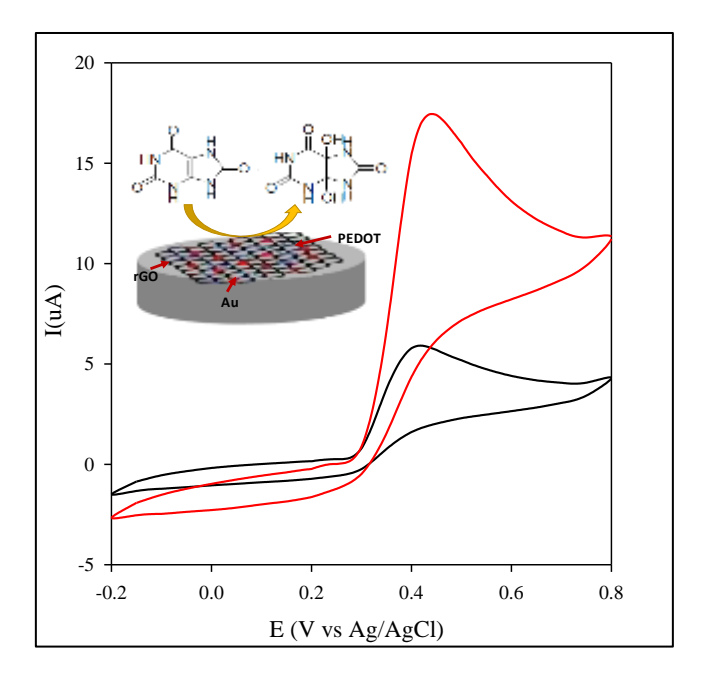


Figure 6. (a) Cyclic voltammograms obtained at the bare GCE (black line) and Au-PEDOT/rGO/GCE (red line) in 0.1 M of PBS (pH 7) containing 1.0 mM of UA. Inset: Electrocatalytic oxidation of UA at Au-PEDOT/rGO/GCE

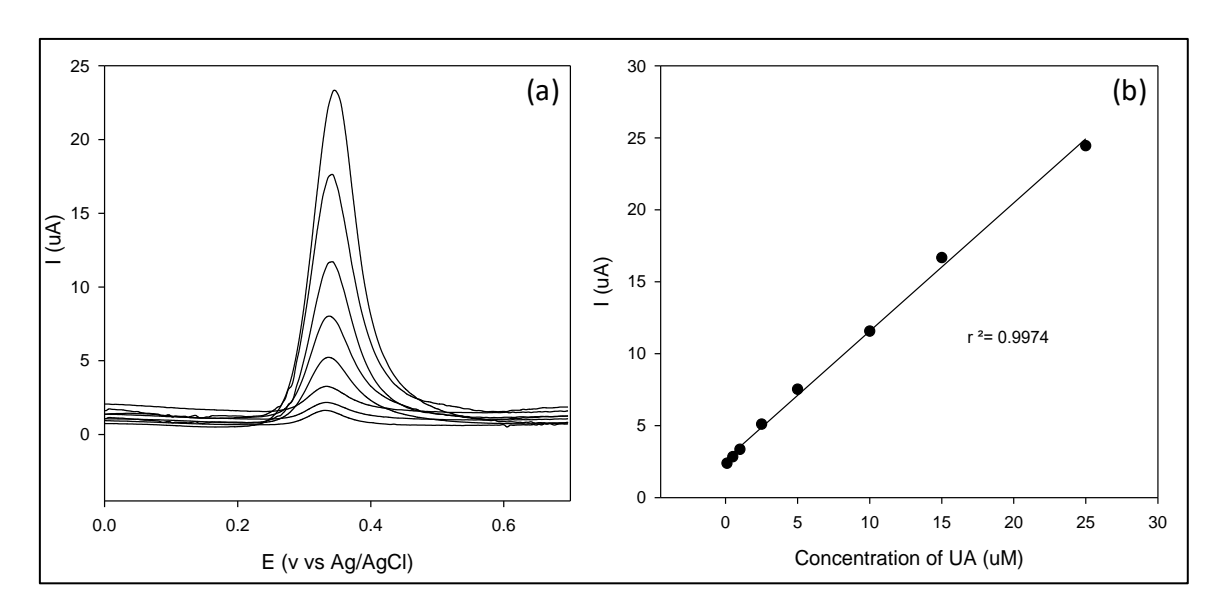


Figure 7. (a) DPV response measured over a range of UA concentration from 0.1  $\mu$ M to 25.0  $\mu$ M and (b) The relationship between the oxidation peaks current against UA concentration

Modified electrode	<b>Type of Detection</b>	Linear Range	Limit of Detection (µM)	Ref
PEDOT/Au	DPV	2.0-600 μΜ	1.50	[25]
Au/rGO/GCE	DPV	6.8-41 μM	1.40	[26]
Au/rGO	SWV	0.5-60 μΜ	0.21	[27]
3D Electrochemically rGO	DPV	0.1-10 μΜ	0.10	[28]
PEDOT/Au hollow nanosphere	DPV	0.15-330 μΜ	0.08	[22]
Au nanocoral/PET	Amperometry	0.2-600 μΜ	0.06	[29]
Au-PEDOT/rGO/GCE	DPV	0.1-25.0 μΜ	0.05	This work

Table 1. Comparison of various type of modified electrode for detection of uric acid in human urine sample

#### Conclusion

In summary, Au-PEDOT/rGO modified electrode has been synthesized by a facile method. The product was characterized by FTIR that observed C-O-C and C-S stretching indicates the PEDOT has successfully presenced in the composite. The morphology of Au-PEDOT/rGO by SEM shows the Au along with PEDOT has attached to rGO sheets. Glassy carbon electrode was modified with Au-PEDOT/rGO and underwent electrochemical characterization by using CV for the detection of UA and shows excellent electrical properties. The detection limit of UA by Au-PEDOT/rGO/GCE in PBS solution is calculated to be 0.05 µM over a linear range of 0.1 µM to 25.0 µM via a DPV studies. The results suggested the great potential use of Au-PEDOT/rGO in selectively non-enzymatic sensing of UA.

#### Acknowledgments

The authors are grateful to Research Acculturation Grant Scheme (RAGS) RAGS/1/2015/ST0/UMT/03/ for financial support as well as Universiti Malaysia Terengganu for providing facilities for undertaking this research.

#### References

1. Yu, H., Zhang, Z., Shen, T., Jiang, J., Chang, D. and Pan, H. (2018). Sensitive determination of uric acid by using graphene quantum dots as a new substrate for immobilisation of uric oxidase. *IET Nanobiotechnology*, 12(23): 191-195.

- Soares, F., Paula, F. D. S., Franco, D. L., Torres, W. and Ferreira, L. F. (2017). Electrochemical detection of uric acid using graphite screen-printed electrodes modified with prussian blue/poly(4-aminosalicylic acid)/uricase. *Journal of Electroanalytical Chemistry*, 806: 172-179.
- 3. Ndrepepa, G. (2018) Uric acid and cardiovascular disease. *Clinica Chimica Acta*, 484(3): 150-163.
- Black, C. N., Bot, M., Peter, G., Snieder, H. and Penninxm B. W. J. H. (2017). Uric acid in major depressive and anxiety disorders. *Journal of Affective Disorders*, 225: 684-690.
- Kand, R., Drábková, P. and Hampl, R. (2011). The determination of ascorbic acid and uric acid in human seminal plasma using an HPLC with UV detection. *Journal of Chromatography B*, 879: 2834-2839.
- Long, Q., Fang, A., Wen, Y., Li, H., Zhang, Y. and Yao, S. (2016). Biosensors and bioelectronic rapid and highly-sensitive uric acid sensing based on enzymatic catalysis-induced upconversion inner filter effect. *Biosensors and Bioelectronic*, 86: 109-114.
- 7. Wei, Y., Liu, Y., Xiu, Z., Wang, S., Chen, B., Zhang, D. and Fang, Y. (2020). Simultaneous detection of ascorbic acid, dopamine, and uric acid using a novel electrochemical sensor based on palladium nanoparticles/reduced graphene oxide nanocomposite. *International Journal of Analytical Chemistry*, 1-13.

- 8. Su, C. H., Sun, C. L. and Liao, Y. L. (2017). Printed combinatorial sensors for simultaneous detection of ascorbic acid, uric acid, dopamine and nitrite. *ACS Omega*, 2(8): 4245-4252.
- 9. Tukimin, N., Abdullah, J. and Sulaiman, Y. (2018). Electrodeposition of poly(3,4-ethylenedioxy thiophene)/reduced graphene oxide/manganese dioxide for simultaneous detection od uric acid, dopamine and ascorbic acid. *Journal of Electroanalytical Chemistry*, 820: 74-81.
- Muhamad, N. B., Khairul, W. M. and Yusoff, F. (2019). Synthesis and characterization of poly(3,4-ethylenedioxythiophene) functionalized graphene with gold nanoparticles as a potential oxygen reduction electrocatalyts. *Journal of Solid State Chemistry*, 275(4): 30-37.
- 11. Li, Y., Du, Y., Dou, Y., Cai, K. and Xu, J. (2017). PEDOT-based thermoelectric nanocomposites- a mini review. *Synthetic Metals*, 226: 119-128.
- 12. Lawal, A. T. (2019). Graphene-based nano composites and their applications. A review. *Biosensors and Bioelectronics*, 2019: 111384.
- 13. Rosli, A. R., Loh, S. H. and Yusoff, F. (2019). Synthesis and characterization of magnetic fe<sub>3</sub>0<sub>4</sub>/reduced graphene oxide and its application in determination of dopamine. *Asian Journal of Chemistry*, 31(12): 2785-2792.
- 14. Berisha, L., Shabani, E., Maloku, A., Jashari, G. and Arbneshi, T. (2020). Electrochemical determination of dopamine and uric acid in blood serum using anionic surfactants at carbon paste electrodes. *Malaysian Journal of Analytical Sciences*, 24(1): 97-106.
- Jin W. and Maduraiveeran, G. (2017).
   Electrochemical detection of chemical pollutants based on gold nanomaterials. *Trends in Environmental Analytical Chemistry*, 14(4): 28-36.
- 16. Harun, N. A., Kassim, S., Tahrin, R. A. A. and Rusdi, N. F. (2018). Bimetallic (Au-Ag) in 3D hot spots as highly sensitive substrate for high performance surface-enhanced raman scattering (SERS). *ASM Science Journal*, 11(1): 86-95.
- 17. Kassim, S., Padmanabhan, S. C., Salaun, M. and Pemble, M. E. (2011). PMMA gold metallodielectric photonic crystals and inverse opals: preparation and optical properties. *AIP*

- Conference Proceeding, 263: 1-4.
- 18. Kaur, M., Kaur, H., and Kukkar, D. (2018). Synthesis and characterization of graphene oxide using modified Hummer's method. *AIP Conference Proceeding*, 1953(1): 030180.
- Johra, F. T. and Jung, W. (2016). Low temperature synthesis of RGO-Au nanocomposite for apparently reduced time and its application as a chemical sensor. *Applied Surface Science*, 362: 169-175.
- Liu, Z., Xu, J., Yue, R., Yang, T. and Gao, L. (2016). Facile one-pot synthesis of Au-PEDOT/rGO nanocomposite for highly sensitive detection of caffeic acid in red wine sample. *Electrochimica Acta*, 196: 1-12.
- 21. Yan, Q., Zhi, N., Yang, L., Xu, G., Feng, Q., Zhang, Q. and Sun, S. (2020). A highly sensitive uric acid electrochemical biosensor based on a nano-cube cuprous oxide/ferrocene/uricase modified glassy carbon electrode. *Scientific Reports*, 10: 10607.
- 22. Ali, A., Zhang, Y., Jamal, R., and Abdiryim, T. (2017). Solid-state heating synthesis of poly(3,4-ethlylenedioxythiophene)/gold/graphene composite and its application for amperometric determination of nitrite and iodate. *Nanoscale Research Letter*, 12(568): 1-10.
- 23. Muhammad, N. B., and Yusoff, F. (2018). The physical and electrochemical characteristic of gold nanoparticles supported PEDOT/graphene composite as potential cathode material in fuel cells. *Malaysian Journal of Analytical Sciences*, 22(6): 921–930.
- 24. Gualandi, I., Tonelli, D., Mariani, F., Scavetta, E., Marzocchi, M. and Fraboni, B. (2016). Selective detection of dopamine with an all PEDOT:PSS organic electrochemical transistor. *Scientific Reports*, 6 (10): 1-10.
- Sekli-belaidi, F., Temple-boyer, P. and Gros, P. (2010). Voltammetric microsensor using PEDOT-modified gold electrode for the simultaneous assay of ascorbic and uric acids. *Journal of Electroanalytical Chemistry*, 647(2): 159-168.

- 26. Wang, C., Du, J. and Wang, H. (2014). A facile electrochemical sensor based on reduced graphene oxide and Au nanoplates modified glassy carbon electrode for simultaneous detection of ascrobic acid, dopamine and uric acid. *Sensors & Actuators: B. Chemical*, 204: 302-309.
- Tian, X., Cheng, C. and Yuan H. (2012).
   Simultaneous determination of L-ascorbic acid, dopamine and uric acid with gold nanoparticles—β-cyclodextrin—graphene-modified electrode by
- square wave voltammetry. Talanta, 93: 79-85.
- 28. Yu, X., Sheng, K. and Shi, G. (2014). A Three-dimensional interpenetrating electrode of reduced graphene oxide for selective detection of dopamine. *The Analyts*, 139: 4525-4531.
- 29. Hsu, M., Chen, Y., Lee, C., and Chiu, H. (2012). Gold nanostructures on flexible substrates as electrochemical dopamine sensors. *Applied Material and Interface*, 4(10): 5570-5575.